Review of the Analysis and Suppression for High-frequency Oscillations of the Grid-connected Wind Power Generation System

Bo Pang, *Member, IEEE*, Qi Si, Pan Jiang, Kai Liao, *Member, IEEE*, Xiaojuan Zhu, *Member, IEEE,* Jianwei Yang, *Member, IEEE,* and Zhengyou He, *Senior Member, IEEE*

***Abstract*—High-frequency oscillation (HFO) of grid-connected wind power generation systems (WPGS) is one of the most critical issues in recent years that threaten the safe access of WPGS to the grid. Ensuring the WPGS can damp HFO is becoming more and more vital for the development of wind power. The HFO phenomenon of wind turbines under different scenarios usually has different mechanisms. Hence, engineers need to acquire the working mechanisms of the different HFO damping technologies and select the appropriate one to ensure the effective implementation of oscillation damping in practical engineering. This paper introduces the general assumptions of WPGS when analyzing HFO, systematically summarizes the reasons for the occurrence of HFO in different scenarios, deeply analyses the key points and difficulties of HFO damping under different scenarios, and then compares the technical performances of various types of HFO suppression methods to provide adequate references for engineers in the application of technology. Finally, this paper discusses possible future research difficulties in the problem of HFO, as well as the possible future trends in the demand for HFO damping.**

***Index Terms*—Damping method, High-frequency oscillation, Stability, Wind power generation.**

I. Introduction

When wind power is delivered by long-distance transmissions or DC converter stations, the grid networks that collect wind power become weak or power-electronic grids from an infinity grid [1]. In this case, the interaction between the wind power generation system (WPGS) and the grid will be formed at the non-fundamental frequencies, which can amplify the small disturbance signals in the system to form the sustaining or diverging non-fundamental frequency components, i.e., the oscillation phenomenon of the grid-connected WPGS. In the early stage of large-scale wind power connected to the grid, the accident cases observed around the world confirmed that low-frequency negative damping characteristics of the power electronic converters in WPGS could lead to the sub-synchronous oscillation (SSO) or sub/super-synchronous oscillation(S^2SO) [2]-[3]. For example, a doubly-fed induction generator (DFIG) based wind farm in Minnesota was connected to the series-compensated grid, which triggered an electrical oscillation of 9.44 Hz, several sub-synchronous oscillations triggered by the interaction between doubly-fed and series-compensated grids, as reported by the Texas Power Regulatory Commission [4], and the sub-synchronous oscillations of 3-30 Hz that appeared in Guyuan, China [5], 27Hz/73Hz S^2SO phenomenon in Hami, China [6].

The frequent occurrence of SSO has drawn the attention of researchers to the problem of high-frequency interactions between wind turbines and power grids [7]-[10]. In contrast to the synchronous generator, which is insensitive to the high-frequency dynamics of the grid, power electronics converter-based WPGS are sensitive to wide-frequency dynamics, including medium and high frequencies (due to the high modulation frequency and wideband coupling of the converter, and the medium-high frequency filtering circuits equipped in the converter), which may interact with the grid in a range of frequencies from one hundred hertz to more than one thousand hertz. In recent years, high-frequency oscillations (HFO) generated by the interaction between wind power systems and power grids have been reported. The frequencies of HFO are generally between 300 Hz and 2 kHz, which confirms that the high-frequency interaction between wind turbine generators (WTGs) and power grids may affect the safe and stable operation of the system. HFO of nearly 1000 Hz was observed in the Borwin1 offshore wind farm in the North Sea, Germany [7], high-frequency harmonic oscillations of 1270 Hz have been observed in the Luxi back-to-back high-voltage direct current (HVDC) project in China [8], resonances of 800 Hz have been observed in an offshore direct-driven wind turbine during AC grid-connected operation [9], and high-frequency harmonic amplification phenomena of 1000 Hz have been observed at Saihanba and Dongshan wind farms in Inner Mongolia in China [10].

Manuscript received March 19, 2024; revised April 30, 2024; accepted May 29, 2024. Date of publication June 25, 2024; Date of current version June 13, 2024.

This work was supported in part by the Fundamental Research Funds for the Central Universities under Grant 2682023CX019, in part by the National Natural Science Foundation of China under Grant U23B6007 and Grant 52307141, in part by Sichuan Science and Technology Program under Grant 2024NSFSC0115. (*Corresponding Author*: *Kai Liao*)

The authors are with the College of Electrical Engineering, Southwest Jiaotong University, Chengdu 610031, China (e-mail: pangbo1025@swjtu.edu.cn; s2018112358@my.swjtu.edu.cn; jiangpan@my.swjtu.edu.cn; liaokai.lk@foxmail.com; zxj@swjtu.edu.cn, jwyang@swjtu.cn; hezy@swjtu.edu.cn).

Digital Object Identifier 10.30941/CESTEMS.2024.00025

2096-3564 © 2024 CES

The occurrence of HFO is highly harmful to both the grid-connected equipment and the power grid. If the oscillation is not severe, the oscillation component is sustaining and will not trigger the protection circuit. The wind turbine can still be in operation, but the negative effects associated with the long-term operation are significant. For the wind turbine, the periodic generator torque pulsation increases mechanical loss, affecting the service life of the generator and increasing the risks of generator failure [11]. For the power grid, the inflow of high-order harmonics into the power system causes increased losses and faster aging of transformers, capacitors, and other power equipment, increasing the risks of power failure. If the oscillation is severe, the oscillation component is diverging, or the oscillation triggers the over-voltage and over-current protection, the wind turbine will be off-grid, which poses a significant threat to the power supply guarantee and safe operation of the power system [12]. Therefore, HFO damping is the basis for efficient power generation and stable operation of the power system.

The research on HFO of wind turbines mainly focuses on analyzing the causes of HFO under various scenarios and developing the suppression methods with high engineering practicability for different working conditions. Unlike the SSO or S^2SO problem, the frequency range involved in high-frequency oscillation is much wider, and the high-frequency oscillation suppression will also be coupled with other problems, such as grid harmonic suppression and dynamic regulation performance of the equipment, which results in the diversity of high-frequency oscillation suppression methods. However, the performance or adaptability of different high-frequency oscillation suppression methods in different scenarios is significantly different. Thus, engineers must mechanistically understand the nature and differences between the many oscillation suppression methods to choose the suitable one for their situation.

In this regard, this paper provides a systematic overview of the modeling, analyzing, and damping for HFO based on the existing research on the HFO of WPGS. This paper is organized as follows. In Section II, the modeling methods of the simplified model applied to the high-frequency characteristic analysis of WPGS are briefly introduced, which is the basis for understanding the occurrence mechanism and damping of HFO. Then, the authors summarize the vulnerable scenarios and occurrence mechanism of HFO and discuss the key of HFO damping in different scenes in Section III. Thereby, the design concept of the existing HFO suppression strategies is presented in Section IV. Also, a comprehensive comparison of the existing HFO oscillation strategies is carried out in this section. Finally, the authors discuss the HFO suppression technology development trend and potential research hotspots.

II. High-frequency Impedance Modelling of WPGS and Its Underlying Assumptions

The work of modeling the characteristics of WPGS was carried out well before HFO received attention. The state-space or impedance models used in analyzing the SSO problems [13] can describe the high-frequency dynamic characteristics of WTGs. The previous research has conducted detailed modeling, revealing valuable conclusions for analyzing the high-frequency dynamic characteristics of WPGS. For instance, it has been confirmed that the dynamics of the PLL (phase-locked loop) can be disregarded when the control parameters of the WPGS are reasonably designed, and the DC voltage control loop has minimal impact on the high-frequency characteristics. By simplifying the high-frequency impedance model of the WPGS as a single-input single-output (SISO) [14] model and neglecting minor factors, the complexity of stability analysis and control parameter design can be significantly reduced. These conclusions emphasize the advantages of the impedance analysis method and lead to the fact that most of the current research on HFO is based on the impedance analysis method.

A. *Basic Assumptions*

Firstly, it is essential to outline several vital assumptions when analyzing the high-frequency dynamics of WPGS. These assumptions aim to identify the factors that need to be considered and those that are negligible in high-frequency impedance modeling.

1) The Control Loop Relates to the Mechanical Components, Such as Pitch Control and Generator Speed Control

The response speed of control loops associated with pitch angle and generator speed is significantly slower than the electromagnetic effects of the generator and converter. This temporal sluggishness translates into low-frequency dynamics in the frequency domain. Typically, the pitch angle adjustment cannot be faster than 10-15 (°/s) [15], requiring at least several seconds to complete the adjustment from a normalized value of 0 to 1. Consequently, the frequency range of pitch control lies below 1 Hz. Similarly, mechanical inertia prevents the rotor speed from rapidly changing, so the mechanical rotor's dynamic cannot influence high-frequency dynamic characteristics.

2) Current Control Loop

The core of the current loop is to track current references. The lower control bandwidth of the current loop means a slower dynamic response speed of the current control, which may cause the dynamic regulation capability of WPGS to fail to meet the grid guidelines. When the control bandwidth of the current loop is over-high, the delay effect caused by the digital control will decrease the control accuracy of the high-frequency signals, which is most typically reflected in the increase of the generator's output harmonics. Therefore, the bandwidth of the current loop is usually limited to no more than one-half of the switching frequency [16]. Thus, the dynamic of the current control loop should be involved in the high-frequency characteristics descriptions of WPGS.

3) Power or Voltage Outer Loop

In typical control systems of WPGS, the control architecture comprises an outer loop and an inner loop responsible for current regulation. The outer loop can manifest as either a power outer loop for wind turbine generators, a DC voltage outer loop for grid-tied inverters, or an AC voltage outer loop for grid-forming wind turbine generators. Within this configuration, the output of the outer loop furnishes control instructions to the inner loop. It is crucial to note that the control logic mandates a discernibly slower response speed for the outer loop than that of the inner loop. Failure to adhere to this requirement could result in the inner loop receiving new current command signals before tracking the previous command, undermining control stability [17]. Extensive theoretical analyses have investigated the relationship between the response speed of the outer loop and that of the inner loop. It is precisely due to this design rationale that the power inner loop or voltage outer loop can be disregarded when scrutinizing HFO.

The author wants to underscore that neglecting the outer loop is predicated on the appropriate parameter design of WPGS. Consequently, any analysis of the small-signal stability issues necessitates the foundation of rational control parameters rather than extreme values. Examining small-signal stability issues using extreme parameters lacks practical significance since it engenders doubts regarding the feasibility of grid connection compliance for WPGS operating under such configurations.

4) Phase Locked Loop (PLL)

The PLL is the essential link in a grid-following DFIG or converter, which tracks the grid voltage phase information to synchronize the generator (or converter) with the grid voltage. Similar to the power or voltage loop, the PLL, as the upper control loop of the current loop, is also a slow response link in the electrical control chain. Compared to the hundreds of hertz of the current loop, the bandwidth of the PLL is currently considered to be controlled within a few tens of hertz around 50 Hz, which is necessary to avoid low-frequency oscillations and transient instabilities in WPGS [18]-[19]. Therefore, when analyzing the HFO of WPGS, it is common practice to ignore the dynamic characteristics of the PLL.

5) Electromagnetic Dynamic Characteristics of Generators or Converters

It can be recognized that whether or not the control links described above should be considered depends on whether the dynamic of the link in high frequency is active. In contrast, the electromagnetic dynamic behavior of a generator or converter as a physical property responds to input signals over the whole frequency range, which means that the dynamic behavior of both generator and converter should be considered over the whole frequency range. However, this does not mean that the electromagnetic dynamic characteristics of a generator or converter cannot be simplified. For instance, from the point of view of the magnitude of the equivalent impedance, the excitation inductance of a DFIG has much less influence on its output impedance than the stator or rotor leakage inductance. From the point of view of the signal input-output linearization, the modulation link of the converter is linear in the range of switching frequencies less than 1/2 [20]. These specific simplifications we will describe in further detail below.

6) Simplification of System Structure

The current mainstream WPGS are DFIG-based WPGS and permanent magnet synchronous generator (PMSG) based WPGS. For DFIG-based WPGS, the DFIG and the grid-side converter (GSC) connect to the grid simultaneously, while the DFIG and the GSC are connected through a common DC bus. For the PMSG-based WPGS, the generator connects to the grid through a back-to-back converter, namely the machine side converter (MSC) and GSC. The MSC is responsible for controlling the generator, while the GSC achieves the connection of WPGS and the grid. The dynamic response characteristics of the DC bus depend on the control links of DC capacitance and DC voltage, resulting in high-frequency signals that are practically difficult to pass through the DC bus [21]-[22]. Therefore, the RSC and GSC of DFIG-based WPGS and the MSC and GSC of direct-drive WTGs are isolated. When analyzing HFO, For the DFIG-based WPGS, the equivalent impedance that interacts with grid impedance is the parallel of DFIG's impedance and GSC's impedance, while for the PMSG-based WPGS, the equivalent impedance is GSC's impedance.

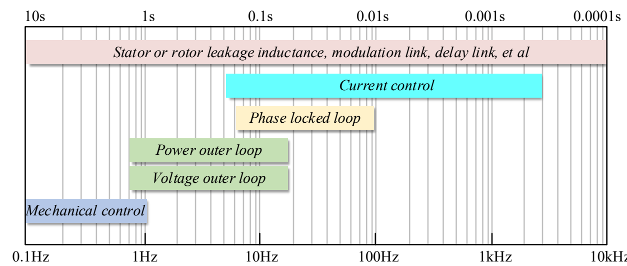

Fig. 1. Distribution patterns of each control link and the dynamic components.

Fig. 1 illustrates the distribution patterns of each control link and the dynamic components across both frequency and time scales. The frequency range of mechanical control is below 1 Hz. The bandwidth of the power or voltage outer loop is in the tens of hertz. The bandwidth of PLL lies within the range of tens of hertz, approximately 50 Hz. The current control loop is currently designed for several hundred hertz. The electromagnetic dynamic behavior manifests across all frequency bands. Considering their frequency distribution and the influence of these control links and dynamic components on the high-frequency dynamic characteristics of WPGS, mechanical control, power or voltage outer loop, and PLL can be disregarded when analyzing HFO of WPG. However, the current control loop and the electrical dynamic characteristics of generators or converters demand consideration.

B. High-frequency Impedance Model of WPGS

Based on the above assumptions, the high-frequency characteristic of WPGS can be regarded as linearized (since the non-linear links PLL has been proved to be negligible and the modulation link of the converter is linear in the range of switching frequencies less than 1/2). Thus, the impedance modeling of WPGS can be deduced in two ways: one is from the physical meaning of the impedance model to construct an equivalent circuit model by treating the individual links as components in a circuit [23]-[25], and the other one is from the definition of the impedance model to derive the analytical expression of the small-signal response of WTGs under small-signal perturbation [26]-[30].

1) Equivalent Circuit Model

In the equivalent circuit model, the converter is regarded as a non-ideal power source with impedance [23]. Since the control inner loops of the converter in WPGS are all current control loops, the converter is essentially a current source [24]. According to the Norton equivalent circuit, the equivalent circuit model of the wind turbine can be described as Fig. 2. (Here, the DFIG-based WPGS is taken as an example.)

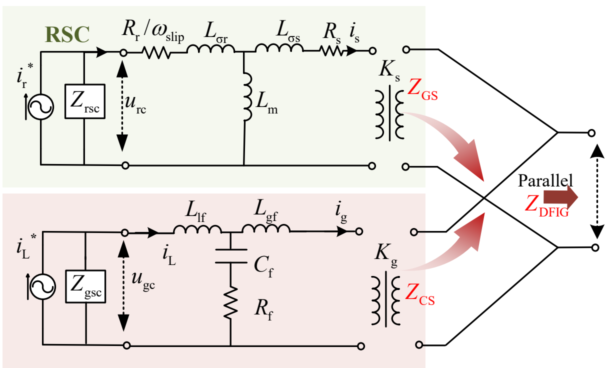

Fig. 2. Equivalent circuit model of DFIG-based wind power generation system.

In Fig. 2, i_r^* and i_L^* are the current reference of RSC and GSC, u_{rc} and u_{gc} are the AC voltages generated by the RSC and the GSC, i_s and i_g are the stator current and GSC's current, Z_{rsc} and Z_{gsc} are the impedance of RSC and GSC, $L_{\sigma s}$ and $L_{\sigma r}$ are the leakage inductance of stator windings and rotor windings, R_s and R_r are the stator resistance and rotor resistance, L_m is the generator excitation inductance, L_{lf} and L_{gf} are the converter side inductance and the grid-side inductance of the LCL filter, C_f and R_f are the filter capacitance and damping resistance. ω_{slip} is the slip angular frequency. K_s and K_g are the transformation ratios of the generator-side and converter-side step-up transformers. The output impedance of the wind turbine Z_{DFIG} is composed of the generator-side impedance Z_{GS} and the converter-side impedance Z_{CS} in parallel. The generator side impedance can be calculated by combining the rotor converter's Norton equivalent model and the generator's T-equivalent model. Similarly, the converter side impedance can be calculated by combining the Norton equivalent model of the GSC and the filter equivalent circuit model. Therefore, obtaining the Norton equivalent models of the RSC and GSC is the key to this modeling approach.

The methods for obtaining the Norton equivalent model of RSC and GSC can be found in [24]. Here, an analysis of RSC is briefly given as an example. Eq. (1) gives the expression of generator rotor voltage in the synchronous speed rotating coordinate system, i.e., the dq frame, where the subscript dq is used to characterize the dq frame. In Eq. (1), 's' is the differential operator in the Laplace domain, H_{ri} represents the rotor current controller (PI controller), H_d represents the control delay, k_{pr} and k_{pi} are the proportionality and integral coefficients of H_{ri}, and T_d is the delay constant, which is approximately equal to 1.5 times the switching delay time [26].

$$\begin{cases} \boldsymbol{u}_{rdq} = (\boldsymbol{i}_{rdq}^* - \boldsymbol{i}_{rdq}) H_{ri}(s) H_d(s) \\ H_{ri}(s) = k_{pr} + k_{pi}/s \\ H_d(s) = e^{-1.5 s T_d} \end{cases} \tag{1}$$

The ratio of the rotor voltage fluctuation to the rotor current fluctuation represents the output impedance of RSC. Thus, the impedance of RSC in dq frame Z_{rsc_dq} can be obtained as follows.

$$Z_{rsc\_dq}(s) = \frac{-\Delta \boldsymbol{u}_{rdq}}{\Delta \boldsymbol{i}_{rdq}} = \frac{-\partial \boldsymbol{u}_{rdq}}{\partial \boldsymbol{i}_{rdq}} = H_{ri}(s) H_d(s) \tag{2}$$

Since the RSC controls rotor current, the slip frequency conversation should be considered from the stator port. Also, considering the frequency offset between the dq and stationary frames, the impedance of RSC in stationary frame Z_{rsc} can be written as (3).

$$Z_{rsc}(s) = \left. \frac{Z_{rsc\_dq}(s)}{\omega_{slip}} \right|_{s=s-j\omega_0} = \frac{H_{ri}(s-j\omega_0) H_d(s-j\omega_0)}{\omega_{slip}} \tag{3}$$

where ω_0 is fundamental frequency of the power grid.

Based on (3) and Fig. 2, the generator-side impedance Z_{GS} can be written as (4). Similarly, the converter side impedance Z_{CS} can be written as (5). For DFIG-based WPGS, its output impedance is the parallel connection of (4) and (5), and for PMSG-based WPGS, its output impedance is (5).

2) Transfer Function Model

In addition to the equivalent circuit model, a feasible way to obtain the equivalent impedance of the WPGS is through the transfer function model. Based on the generator electromagnetic transient model [27], the transfer function equation of the generator's stator current is described in Fig. 3.

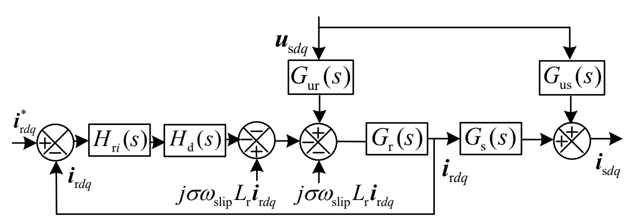

Fig. 3. Transfer function model of generator side for DFIG-based wind power generation system.

$$Z_{GS} = K_s^2 \left[\frac{sL_m \left(\frac{H_{ri}(s-j\omega_0) H_d(s-j\omega_0)}{\omega_{slip}} + sL_{\sigma s} + R_s + sL_{\sigma r} + R_r \right) + (sL_{\sigma s} + R_s) \left(\frac{H_{ri}(s-j\omega_0) H_d(s-j\omega_0)}{\omega_{slip}} + sL_{\sigma r} + R_r \right)}{\frac{H_{ri}(s-j\omega_0) H_d(s-j\omega_0)}{\omega_{slip}} + sL_{\sigma r} + R_r + sL_m} \right] \tag{4}$$

$$Z_{GC} = K_g^2 \left[\frac{(1 + sC_f R_f)(H_{gi}(s-j\omega_0) H_d(s-j\omega_0) + s^2 C_f (L_{lf} + L_{gf}) s^2 L_{gf} C_f (H_{gi}(s-j\omega_0) H_d(s-j\omega_0) + sL_{lf}}{sC_f [H_{gi}(s-j\omega_0) H_d(s-j\omega_0) + sL_{lf} + R_f] + 1} \right] \tag{5}$$

In Fig. 3, G_r, G_s, G_{ur}, and G_{us} are the intermediate variables calculated using the voltage and flux equations of the asynchronous generator. Their expressions are written as (6).

$$\begin{cases} G_r(s) = 1/(R_r + \sigma s L_r) \\ G_s(s) = -L_m / L_s \\ G_{ur}(s) = L_m(s + j\omega_{slip}) / L_s(s + j\omega_0) \\ G_{us}(s) = 1/[L_s(s + j\omega_0)] \end{cases} \tag{6}$$

As thus, the transfer function of stator current in dq frame $\boldsymbol{i}_{sdq}$ can be written as (7), in which H_{EV} represents the dynamic control performance of fundamental current, Y_{GS_dq} represents the response component of stator current under the perturbation of stator voltage [28]-[30]. With this physical significance, it is easy to notice that Y_{GS_dq} is the generator-side equivalent admittance in the dq frame.

$$\boldsymbol{i}_{sdq} = H_{EV}(s)\boldsymbol{i}^*_{rdq} + Y_{GS\_dq}(s)\boldsymbol{u}_{sdq} \tag{7}$$

With the frequency conversion based on Y_{GS_dq}, the generator side impedance expression of DFIG obtained is the same with (4). Similarly, based on the equivalent transfer function of the GSC, the equivalent impedance on the GSC side can also be derived, which is consistent with (5).

III. Vulnerable Scenarios and Occurrence Mechanism of High-frequency Oscillation

According to the impedance stability analysis theory [31], the stability of a SISO interconnected system is determined by the phase difference between the two sub-systems at the impedance magnitude intersection. The interconnected system is unstable if the phase margin at the impedance magnitude intersection location is insufficient. Therefore, it is necessary to introduce the high-frequency impedance characteristics of the WPGS before analyzing the occurrence mechanism of HFO.

The impedance curve of a 2MW DFIG-based WPGS with an LCL filter is given in Fig. 4 as an illustration, in which the parameters of the 2 MW DFIG are shown in Appendix A. In Fig. 4, the impedance curve is classified into four regions according to its phase characteristics (The detailed analysis for the impedance in different regions can refer to [23]-[24]).

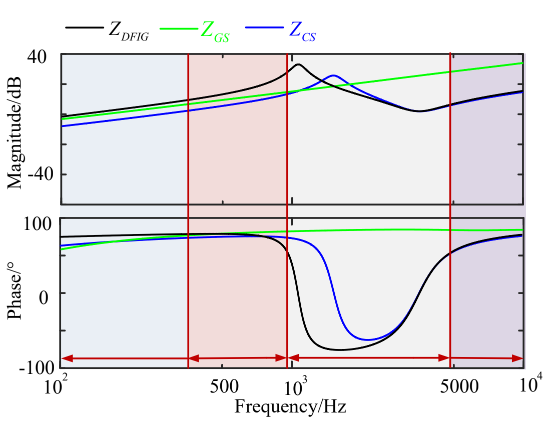

Fig. 4. Impedance curve of a 2 MW DFIG-based WPGS with LCL filter.

Table I describes the impedance characteristics in Fig. 4. It can be seen in Table I that there is no apparent negative damping region in the high-frequency impedance of the WPGS, but there is a possibility of an underdamped region, i.e., region B. In region B, the equivalent resistance provided by the proportionality link of the PI controller is much smaller than the generator inductance and the converter-side inductance of the LCL, resulting in the overall impedance of the WPGS presenting as close to a purely inductive one, which makes this region a potential risky region. As the frequency increases, the LCL filter capacitance (and resistance) and the LCL grid-side inductance successively play a role, and regions C and D occur. Regions C and D are the extensions of region B, which is the product of the influence of the impedance difference of the LCL filter in different frequency bands. For instance, the impedance of the WPGS equipped with an L filter does not have region C and region D.

TABLE I
TYPICAL IMPEDANCE CHARACTERISTIC OF WPGS IN HIGH-FREQUENCY

Region	Impedance characteristics	Influencing factors
A	Inductive + Resistive	Generator inductance Inverter side inductance of LCL Proportionality link of PI Integral link of PI
B	Inductive	Generator inductance Inverter side inductance of LCL Proportionality link of PI Control delay
C	Capacitive+ Resistive	Generator inductance Inverter side inductance of LCL Proportionality link of PI Control delay Capacitance and resistance of LCL
D	Tend to be inductive	Generator inductance Grid side inductance of LCL Proportionality link of PI Control delay

It can be summarized from the above description that the occurrence of HFO in WPGS requires the grid to behave significantly capacitive or negatively damped. This means that HFO usually does not occur when the WPGS is connected to a conventional inductive weak grid or a weak grid with series compensation. In the former case, the grid behaves purely inductive; in the latter case, the grid may behave capacitively. However, the capacitive region is in the low-frequency region [32], which is more prone to induce SSO or S^2SO rather than HFO [33]. Thus, the vulnerable scenarios from which HFO can be concluded are described in Fig. 5.

A. HFO Scenario 1: The WPGS Connects to a Shunt Compensated Weak Grid

Shunt compensation is one of the most commonly used reactive compensation methods for power systems to improve voltage quality [34], of which shunt capacitors are the most economical and practical means. When the shunt-compensated grid shows a significant capacitance in the high-frequency band, the high-frequency interaction between the grid and the WTGs may induce HFO.

For the HFO phenomenon in this scenario, existing studies have conducted more in-depth research on the factors influencing the occurrence of oscillations. For example, [35]-[36] analyzed the influence of the voltage control and current control loop on the system's high-frequency stability and pointed out the current loop's strong influence and the voltage loop's weak influence. [37] analyzed the grid-connected stability of the large-scale (MW-class) and the small-scale kW-class WPGS and found that both the MW-class and the kW-class units face HFO risk. However, the proportional link of the current loop controller significantly influences the HFO of MW-class WPGS. In contrast, the high-frequency impedance characteristics of kW-class WPGS are less affected by the current controller parameters. [38] analyzed the impact of unit capacity and number of units on the high-frequency stability of the system and found that the unit capacity not only affects the oscillation frequency but also impacts the DFIG phase, leading to changes in oscillation amplitude. Although PLL is generally considered to be irreverent to HFO, some studies [39] discussed the role of PLL in depth when the mechanism of HFO oscillations was not yet precise. The conclusion is that only when the design of the PLL bandwidth exceeds the normal design by more than ten times can the PLL negatively affect the high-frequency stability of the system. To comprehensively and systematically analyze the influence of each factor on the high-frequency stability, the participating factor method was employed to quantitatively assess each influencing factor's contribution to the HFO [40]-[41].

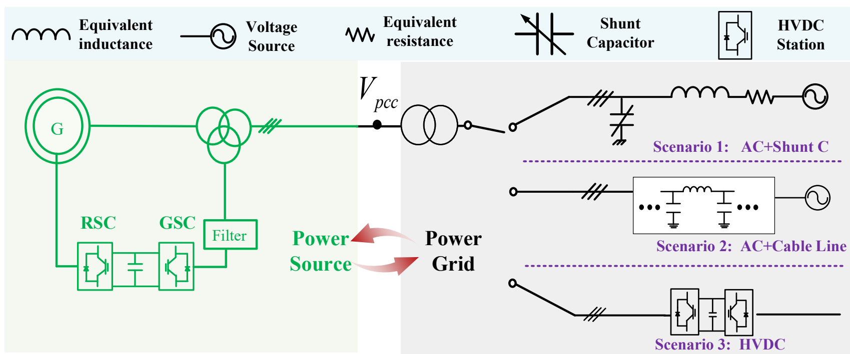

Fig. 5. Impedance curve of a DFIG-based WPGS with LCL filter.

The occurrence mechanism of the HFO in this scenario can be explained as follows. Due to the combined effect of the current controller and the generator inductance (and the LCL inductance), the high-frequency impedance of WPGS is close to inductive, while the shunt-compensated grid is capacitive in high frequency. This phenomenon creates an oscillation like the LC resonance. Based on this mechanism, some studies further discussed the oscillation characteristics in this scenario. [23] tested the high-frequency oscillation characteristics of the grid-connected WPGS with different grid strengths, shunt compensation degrees, converter control parameters, and generator speeds. [42] discussed the mechanistic difference between the divergent and persistent oscillations in this scenario, i.e., whether the phase difference is more than 180° or not, and analyzed the oscillation due to the control delay contribution of divergence, [43] analyses the HFO phenomenon faced by three-phase-four-wire grid-connected devices and extends the oscillation mechanism analysis method to zero-sequence loops. [44]-[45] discussed the frequency shifts of HFO caused by changes in grid strength and shunt compensation capacitor. The general conclusion is that as the grid strength decreases and the degree of parallelism increases, there is a significant decrease in the oscillation frequency [46].

B. HFO Scenario 2: The WPGS Connects to the Grid via a Long AC Cable

At some point, the grid may exhibit significant capacitive impedance characteristics due to using AC cables even without shunt compensation, e.g., offshore wind power connected to the grid via submarine cables or on-road wind power connected to the grid using power cables [47]. In such scenarios, the presence of the AC cable makes the grid impedance capacitive in several frequency bands, and the grid impedance amplitude shows periodic peaks. The complex grid impedance characteristics make HFOs in this scenario receive special attention, especially the effect of AC cable characteristics on the high-frequency stability of the system, which is the core of such HFOs. For example, [48] discussed the equivalent impedance modeling of AC cable, proposed a cable equivalent impedance resolution method based on Π circuit and iterative method, and pointed out that the longer the AC cable is, the lower the oscillation frequency is. [49]-[51] analyzed the effects of the equivalent inductance [49], parasitic capacitance [50], and parasitic resistance [51] on the oscillation characteristics. [52] used the vector fitting method to model the AC cable, then found the conclusion that when the number of wind turbine units increases, the risk of instability increases, and when the length of the cable increases, the oscillation frequency decreases. [22] researched the aggregated modeling of a multi-WTG distributed access grid system, considering the transmission cables between WTGs.

The mechanism of the HFO in this scenario is the same as that of the HFO in scenario 1, but the oscillation characteristics are different. The HFO of the WPGS connected to the shunt-compensated grid usually has only one oscillation mode, whereas when the WPGS is connected to the grid with an AC cable, due to the multi-resonant peak of the grid impedance, the HFO may have multiple oscillation modes. The multi-modal HFO phenomenon, i.e., the simultaneous existence of oscillatory components at multiple frequencies in the system, was reported by [53]. Further, [54] theoretically explains this multi-modal HFO phenomenon based on the multi-terminal Π-equivalent analysis of a long-distance transmission cable.

It should be noted that the HFOs in both scenario 1 and scenario 2 are essentially the resonant effects of inductive and capacitive links. These two types of HFOs are also referred to as HFR in the vast majority of cases, and they do not exhibit a diverging characteristic because they are essentially underdamped rather than negatively damped. However, when the WPGS control delay is not well handled, such as when the proportional link parameter in the control loop is too large, unexpected negative damping [42] may occur, resulting in the diverging of oscillation.

C. *HFO Scenario 3: The WPGS Connects to the Grid via HVDC Station*

Using a HVDC station to collect wind energy is a vital method for the grid to utilize large-scale wind energy, especially in China [55]-[56]. As a power electronic device, the HVDC converter may show capacitive or even negative damping characteristics in the high-frequency when its control structures, control modes, and control parameters flexibly vary. Thus, the WPGS connected to the HVDC will also face the risk of HFOs [57].

Unlike the passive grids in scenarios 1 and 2, such active grid usually has a complex impedance characteristic. The commonly used structures of HVDC are the two-level voltage source converter (VSC)-based HVDC and modular multilevel converter (MMC)-based HVDC. Existing studies have demonstrated that both impedances are approximate [58]-[61] in high frequency, and the structural differences between the two can be ignored when analyzing HFO problems. For example, [58] analyzed the similarities and differences between the impedance curves of VSC-HVDC and MMC-HVDC, and the impedance characteristics of MMC in the low-frequency band are more complicated due to the circulating current and voltage equalization control, and the two are almost the same in the high-frequency band. In the specific HVDC impedance modeling, based on the reasonable neglect of the control loop, [59] clarified that the HVDC impedance could be linearly modeled as a transfer function of the terminal voltage and the output current, and [60] proposed the equivalent circuits methodology for describing the dynamic characteristics of the VSC-HVDC and the AC grid, which consists of several partitioned sub-systems, such as converter station converter and the grid. [61] proposed a model step-down method based on the normalized sensitivity index, which provided a sufficient theoretical basis for the simplified process of HVDC high-frequency impedance.

The impedance modeling of HVDC provides a strong foundation for the discovery of the mechanism of HFO. Harmonic resonance modal analysis (HRMA) based on the admittance matrix [62] can effectively analyze the source of oscillation (oscillation induced by the critical unit). [63] analyzed the high-frequency oscillation mechanism when the wind farm is connected to the HVDC converter station, and pointed out that the high-frequency impedance of the converter station has a periodic negative damping characteristic, in which the voltage-loop control delay of the HVDC station is the key to lead to this phenomenon. [64] discussed the high-frequency stability of the HVDC system with different control delays and control parameters. Then, it clarified the effect of the voltage-loop control parameter on the oscillating characteristics (The larger the voltage-loop proportional parameter is, the worse the stability is, and the integral parameter has little effect). In [65], the eigenvalue analysis is employed to determine the oscillation modes, and the sensitivity analysis is used to determine the participation factor. The analysis in [65] reveals the mechanism of oscillation more comprehensively, i.e., the control change delay of the wind farm side VSC (WFVSC) introduces the negative damping at high frequency, resulting in the overall system presenting the negative damping.

In practical engineering, the offshore wind farm may connect to an HVDC converter through the submarine cables, so scenario 3 may also include the AC cables of scenario 2 (this scenario is notated as scenario 3*). In this scenario, the simultaneous existence of resonance peaks in AC cable and negative damping in HVDC, increases the risk of oscillations. [66] reported that the MMC-HVDC high-frequency band of the Yu’e DC has a significant negative damping and that the MMC-HVDC high-frequency band has a significant negative damping. Band has a significant negative damping effect, and the presence of cable further increases the risk of high-frequency instability. The impedance modeling and oscillation mechanism analysis in this case are also well handled, which is essentially an extension of the previous work. In [67]-[68], the high-frequency characteristics of HVDC including AC cable are modeled. [69]-[70] analyzed the high-frequency damping characteristics under the coupling of the cable and the HVDC control and clarified that the traditional control delay elimination or inefficiency can only eliminate the negative damping but cannot provide further positive damping.

Table II summarizes the three typical HFO scenarios described above. It delineates the characteristics, morphologies, and causative factors of high-frequency oscillations occurring in each of these scenarios.

IV. Categorization, Comparison, and Summary of the Different HFO Damping Technologies

Oscillation is a product of the interaction between the power source and the power grid in the interconnected system, so oscillation-damping measures added to both the power source and the grid side are theoretically feasible. As shown in Fig. 6, the oscillation damping measures can be classified

TABLE II
TYPICAL CHARACTERISTICS OF THE HFO IN DIFFERENT SCENARIOS

Scenario	Oscillation characteristics	Modal	Interaction Mechanism		Ref
			Power source	Power grid	
Scenario 1	Persistent	Single	***Inductive***: generator inductance, inverters sider inductance of LCL and current control loop	***Capacitive***: the shunt-compensated capacitor	Impedance modeling and analysis:[35]-[41] HFO occurrence Mechanism: [42]-[46]
Scenario 2	Persistent	Multi	***Inductive***: generator inductance, inverters sider inductance of LCL and current control loop	***Capacitive***: the parasitic capacitors of the long transmission cables	Impedance modeling and analysis:[[48]-[52] HFO occurrence Mechanism: [53]-[54]
Scenario 3	Divergent	Single	***Inductive*** (+resistive): generator inductance, inverters sider inductance of LCL and current control loop	***Negative damping***: the control delay of the control of WFVSC	Impedance modeling and analysis:[[66]-[68] HFO occurrence Mechanism: [69]-[70]
Scenario 3*	Persistent & Divergent	Single & Multi	***Inductive*** (+resistive): generator inductance, inverters sider inductance of LCL and current control loop	***Negative damping+ Capacitive***: the control delay of the WFVSC, the parasitic capacitors of the long transmission cables	

into three main categories according to the implementation location: active control by additional devices, passive control by additional devices, and active control of WPGS.

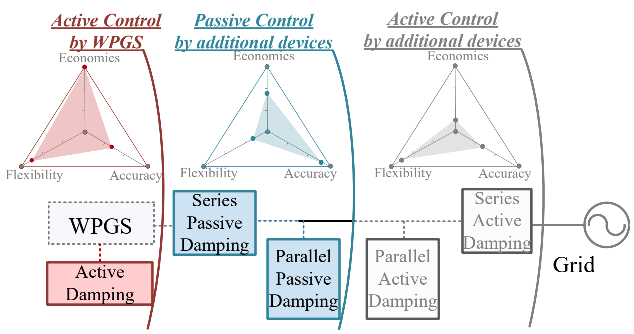

Fig. 6. Classification of oscillation damping measures.

For the first type of oscillation damping scheme, additional damping is generated by the additional active devices such as static var generator (SVG), static synchronous compensator (STATCOM), or energy storage converters to improve the overall damping level of the system[71]-[72]. Due to the high cost of SVG, STATCOM, etc., the introduction of additional active devices for HFO damping alone does not satisfy the requirements of the engineering economy. Therefore, this type of scheme is usually applied to scenarios where SVG or energy storage plants are already constructed [73]. In addition, the additional damping control of SVG or energy storage converter is similar to the active damping control technology of WPGS converter, which will be introduced in detail subsequently, so this paper does not elaborate on this technical scheme.

The second type of oscillation damping scheme is based on passive devices, where the impedance characteristics of the system are regulated by adding various filters and dampers. An in-depth study on the design of passive dampers has been carried out in the existing literature. [74] systematically analyzed typical passive filters' design principles, advantages, and disadvantages. Also, in [74], the second-order dampers were designed, and the principles of applying resistance, capacitance, and inductance in passive damper design were discussed. The application of series blocking and bypass filters in HFO suppression induced by WPGS access to the grid via cable was discussed in [75]. An RLC series blocker was designed to damp HFOs caused by WPGS connected to the HVDC in [76]. [77] designed a high-order filter containing multiple trap loops to suppress oscillations and proposed a general design method for the parameters of this type of filter. In [78], a C-type filter was designed based on a series RC filter, which can provide better highpass characteristics and high-frequency damping to the system. Overall, the advantages of passive damping are that the technology is mature, simple to implement, and reliable, while the disadvantages are that the damping characteristics are fixed once the design is completed, which means the passive damping is not flexible enough. Meanwhile, passive damping will increase the system power loss and heat, which generates additional economic costs to the users of grid-connected equipment or power grid [79]-[80].

The core of the third type of oscillation damping method is to make full use of the converter's wideband regulation capability in the WPGS. In this control concept, the WPGS generates a 'virtual impedance', which can be actively involved in the damping control of the system. This technique has significant economic advantages over the first two options, as it does not require the introduction of additional equipment and does not generate additional power losses. Like the first scheme, the 'virtual impedance' created by modifying the converter control loop can be dynamically and flexibly adjusted, which allows the WPGS to cope with different HFO scenarios without modifying the hardware [81]. It is essential to point out that the active control capability of the WPGS is limited and susceptible to disturbances, and its control performance is affected by the switching frequency of the converter, the control delay, and the power consumption of the converter.

Overall, the performance of the three types of technical solutions differs in terms of economy, flexibility, and accuracy of damping control. As shown in Fig. 6, oscillation suppression methods based on active control generally have high flexibility but limited control accuracy, and oscillation suppression methods based on additional devices are relatively less economical and require additional spending or losses. Among these three technically feasible solutions, the active control of WPGS is the exploitation and utilization of the new energy power control potential, which is the key to the improvement of power source regulation's capability under the development trend of large-scale new energy, and the focus of the research on HFO damping technology.

Next, this paper will provide a technical overview of HFO damping methods based on active control, categorized in a way oriented towards control objectives, to clarify the design intent of different oscillation suppression methods.

A. Classical Method: HFO Damping Based on the Resonator

The traditional approach is to reshape the impedance of WPGS at a single-frequency point impedance by a resonator, which was previously widely used in harmonic suppression or SSO damping. The resonator is essentially an AC signal controller at a specific frequency. Any form of resonator needs to specify the operating frequency, i.e., when applying a resonator for oscillation damping, the oscillation frequency must be inputted to the controller, which can be either a fixed value set by a human in advance or a dynamic value provided by the oscillation frequency detection link. For example, in [42] and [82], the oscillation frequency is obtained in advance by theoretical analysis (the oscillations were considered to be at a fixed frequency). The oscillation frequency can also be obtained in real-time using the adaptive notch filter (ANF) [83], sliding rectangular window [84], etc., as thus the resonant controller can dynamically adapt to the changes of the oscillation mode [85]-[86]. However, the practicality of this impedance reshaping method based on frequency detection is also unsatisfactory due to its poor working mechanism. This method works effectively only when the oscillation occurs and is sufficiently pronounced (such that the oscillation frequency can be accurately detected). This 'post-event' response mechanism is constrained by the frequency detection performance on the one hand, which is unable to respond to the change of oscillation frequency in time [54], [87], and on the other hand, it is unable to avoid over-voltage and over-current phenomena of the device in time.

B. Wideband HFO Damping Method

For the HFO under scenario 1, when the degree of shunt compensation is changed, the oscillation frequency is shifted widely, making the oscillation suppression based on the resonator ineffective. The HFO under scenario 2 may have multiple oscillation modes simultaneously, so multiple resonance suppressors and their parameters must be co-designed, making the control complicated. Therefore, many studies have realized that a key to improving the effectiveness of oscillation damping is to make the damping controller effective over a wide bandwidth.

The simplest wideband oscillation damper is the virtual impedance effective over the whole frequency range. This kind of virtual impedance can be achieved through a proportional link of voltage feedforward or current feedback. For example, [88] introduced virtual resistance through current feedback in GSC, and [89] implemented stator voltage feedforward proportional control in DFIG to increase the equivalent resistance of the generator. [90] further considered the effect of the control delay on the virtual resistance in the digital discrete process and designed the virtual resistance with a series delay compensation link. However, the whole-band virtual resistance ignores a critical issue that it affects both the low-frequency characteristics and the fundamental frequency characteristics of the WPGS, with the former affecting the performance of the possible SSO damper and the latter directly affecting the large-signal stability, dynamic regulation characteristics, etc. of the WPGS. Therefore, the wideband oscillation suppressor should be effective in the frequency range where 'there is a need for HFO oscillation damping' rather than in the whole frequency range.

Further, various improved wideband controllers have been developed, the core idea of which is to artificially control the bandwidth of the virtual impedance using a high-pass filter or an overshooting hysteresis controller. [91] developed a high-pass virtual impedance with high-pass filtering and proportional link, introducing a virtual resistance that is only effective in the high-frequency range. Thereby, [92] optimized the control parameters based on this by taking into account the effect of the control delay. [43] developed an oscillation suppressor based on second-order high-pass plus second-order differential, which enhances the isolation of high-frequency signals from the fundamental frequency signals. [23] replaced the proportional link with an integral or differential link based on the high-pass filter, and changed the virtual resistor into a virtual negative inductance and a virtual positive capacitance, which enhances the impedance reshaping effect. In addition to the high-pass filter, the lead-lag controller [93] can be employed as a filter to extend the effective frequency range of the virtual impedance. Thereby, [54] developed a high-order lead controller to achieve the impedance phase adjustment in the wide frequency range of the WPGS, and [87] designed the series dual lead-lag controller, which can be adjusted by adjusting the cut-off frequencies of the two independent over-advanced lag controllers, changing the oscillation damping frequency range and phase adjustment strength.

Considering the frequency range in which HFOs may occur, the WPGS also needs to deal with harmonic currents (which are mandatory by the grid-connection guidelines). Suppose harmonic suppression is not adequately considered during HFO suppression. In that case, it may lead to incompatibility between stability enhancement and power quality enhancement, e.g., when the virtual negative inductance [85] is used for oscillation damping, the virtual negative inductance reduces the impedance amplitude of the WPGS, increasing the harmonic current. Relevant researchers have proposed solutions based on improving the damping controller or adjusting the control scheme. [44] adopted the idea of virtual high-pass resistors connected in parallel with resonators, the former is used to suppress HFOs, and the latter is used to eliminate current harmonics. [45] synthesized the demand for oscillation suppression and harmonic current suppression on the impedance characteristics of the WPGS, and makes it clear that the core of HFO damping lies in lowering the phase of the WPGS impedance, and the core of harmonic current suppression lies in increasing the impedance amplitude of the WPGS. Then, a virtual variable frequency resistance (VFR) based on the Chebyshev filter was designed. In addition to the modifying of damping controller, [94] focused on the DFIG-based WPGS, fully exploited the regulation potential of the dual converter, and designed the idea that one converter is used to cope with the oscillation issue, and the other is used to eliminate harmonic currents.

Fig. 7 provides a comprehensive overview and classification of HFO damping methods. The full frequency band controllers are proposed to address the issue of traditional HFO suppression methods not being applicable in scenarios with oscillation frequency shifts and multiple oscillation modes. However, these approaches impact the low-frequency and fundamental characteristics of WPGS, possibly affecting the performance of SSO dampers, large signal stability of WPGS, and dynamic adjustment characteristics. Consequently, the controllable frequency band HFO dampers are proposed. In addition, the above methods don't consider the compatibility between stability enhancement and power quality enhancement, and the HFO oscillation suppression methods that take into account harmonic suppression are further constructed.

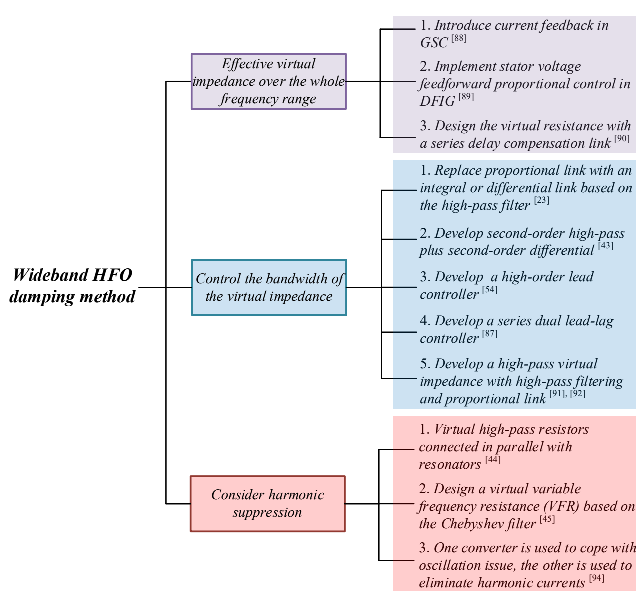

Fig. 7. Classification of wideband HFO damping method.

C. Oscillation Damping Control Adapted to Changes in the Parameters of WPGS.

In addition to developing wideband damping, HFO damping research focuses on how the damping controller adapts to the offset of the unit parameters. Since the passive components of WPGS, such as generator inductance, generator resistance, filter inductance, capacitance, etc., have a significant impact on the high-frequency impedance of WPGS, the saturation effect, skin effect, and aging of the devices during the operation of the WPGS will make the WPGS parameters grasped by the User inaccurate, which makes it difficult to give full play to the efficacy of the oscillation damping controller.

Introducing robust control into the design of damping controller or control parameters is an effective means to ensure the effect of oscillation damping when the parameters of WPGS change, in which the more commonly used method is the optimal control based on H_∞. [95] constructed an oscillation damping using the H_∞ optimal design method, which is still based on voltage feedforward or current feedback but takes the controller as an unknown quantity to be solved. The H_∞ optimal design can solve the controller expression that meets the desired objective through the paradigm calculation. Robust controllers for VSCs with LCL filters were designed by [96] to improve system damping, and robust controllers for converter impedance phase adjustment and amplitude correction were designed by [97] and [98], respectively. Similarly, H_∞ current controllers for regulating DFIG impedance replication were designed by [99], and H_∞ impedance reshaping was designed [100] for GSC to solve HFO in the frequency below 1000 Hz.

In addition to the case of WPGS parameters varying, when the number of units requiring impedance reshaping is large, engineers may also have to be troubled by frequent debugging of oscillation suppression parameters, especially when the capacity or parameters of these units are significantly different. Relevant researchers have found that, for VSCs, the impedance reshaping effect of voltage feedforward control is independent of the unit's original parameters, if the VSC employs an L filter, or the VSC uses the LC or LCL filter while controlling the grid-side currents [101]. Therefore, some generic damping controllers have been developed. For example, [102] proposed a VSC impedance reshaping controller based on grid voltage feedforward, where the controller does not suffer from performance degradation after being applied to units of different capacities. According to the T-equivalent circuit of DFIG, the DFIG resembles a VSC that employs an LCL filter and controls the current on the converter side (the capacitor branch is the excitation branch). Thus, direct voltage feedforward control of the DFIG cannot achieve the effect in [102]. The solution to this issue is to adjust the control structure of the DFIG. For instance, [103] designed a feedforward controller for DFIGs with LC filters at the machine side, and [104] designed an oscillation damping controller to change the power generation control of the DFIG from stator current control to rotor current control. In any case, these methods are more applicable to newly built WPGS. For WPGS that are already in operation, these oscillation suppression methods, which require changes in the original control structure, are hard to make oscillation suppression any easier.

In order to enhance the reader's comprehension of the distinctions among the different types of controllers mentioned above, Table III is presented to provide a comprehensive comparison of strategies for HFO suppression which applied in WPGS.

D. Oscillation Suppressor Based on HVDC Active Control

When WPGS connects to the grid via an HVDC station, oscillation damping via WPGS can still be effective. However, oscillation damping imposed on the HVDC side is usually considered more economical. According to the aforementioned HFO mechanism under scenario 3, it is clear that the negative damping introduced by the HVDC converter is the key to the system instability, in which the control delay of the HVDC converter is the core of causing the negative damping. Hence, the HFO damping under this scenario mainly revolves around attenuating or eliminating the influence of the HVDC converter's control delay on the impedance of the HVDC side. Attaching a filter to the sampling signal or control loop is a feasible and effective way. Understood from an impedance perspective, this can be thought of as reducing the bandwidth of the control loop, thus avoiding the introduction of negative high-frequency damping in the control loop. For example, [105] added a bandpass filter to the voltage feedback loop so that only the fundamental frequency components can enter the control system, and [65] added first-order lowpass filtering to both the voltage and current loops, [63] plants the lowpass filter in the voltage feedforward loop and the proportionality link of the PI controller. However, the nature of the above lowpass filtering-based oscillation suppression is to avoid the negative effect of control delay by reducing the controller bandwidth, which inevitably affects the HVDC dynamic performance. This issue can only be addressed in the design of the filter form and parameters [106], and it is difficult to solve it completely. Besides, compensating the signal delay based on phase lead control can also mitigate the effect of control delay. For example, in [107], a delay compensation link is added to the signal in the feedback loop to attenuate the effect of control delay on the impedance characteristics of the HVDC, and in [64], an analytical expression for a voltage controller that can counteract the effect of the control delay is derived based on the grid voltage feedforward.

As described in Section III C, the WPGS may connect to the HVDC station via an AC cable, at which point, in addition to the negative damping of the HVDC, the AC cable is also a potential causative factor for the HFO. Since these two potential causes are not coupled, the countermeasures are usually independent. It should be noted that introducing positive damping is necessary for coping with the HFO caused by AC cable. However, the significant control delay of HVDC makes the virtual impedance control of HVDC challenging to design [58]. So, the passive damping method is usually adopted when using HVDC to solve the potential HFO risk brought by the AC cable. For example, [108] constructed an additional passive damping based on the LC-parallel R passive damping. Similarly, in [70] and [109], passive damping is designed as a series RLC and a resonant-RL. In these controls, active and passive controls are independent of each other, in which active control is responsible for eliminating the negative damping effect, and

TABLE III
SUMMARY OF HFO SUPPRESSION METHODS APPLIED IN WPGS

Name	Implementation		Performance		
	Implemented target	Controller type	Wide frequency	Compatibility with harmonics suppression	WPGS parameters robust
Resonant damper	Impedance reshaping at a single-frequency	Resonator [42], [82]-[86]	×	×	×
Wideband HFO damper	Whole frequency effective	Proportional controller [88]-[90]	√	×	×
	Partial frequency effective	1. High-pass filter + proportional controller [91]. 2. Second-order high-pass filter + second-order differential controller [43]. 3. High-pass filter + integral or differential controller [23]. 4. High-order lead controller [54]. 5. Series dual lead-lag controller [87].	√	×	×
	Simultaneously damp HFO and suppress the harmonics	1. Virtual high-pass resistors + resonators [44]. 2. Chebyshev filter [45]. 3. Dual converter [94].	√	√	×
HFO damper adapted to changes in the parameters of WPGS	Adapt to the offset of the unit parameters	1. Robust controller [95]-[100]. 2. VSC voltage feedforward-proportional controller [102]. 3. DFIG Capacitor current feedback-low pass filter + proportional controller [103]. 4. DFIG voltage feedforward-lead-lag controller [104].	√	×	√

passive control enhances the positive damping for the interconnected system.

V. Outlook for Future Research on HFO of WPGS

The further development of wind power generation is an inevitable trend, and as the status and role of WPGS in the power system changes, the access methods, operation modes, and performance requirements of WPGS will be updated. Thus, whatever means of analyzing and damping HFO are time-sensitive at a macro time scale. The authors believe that the focus of future HFO research in wind power generation may be the following aspects.

Most currently reported techniques for analyzing and suppressing high-frequency oscillations in WPGS are oriented to linear control (vector control) based units. As the proportion of WPGS in the grid increases, the grid puts forward higher requirements on the operating capability of WPGS, and high-performance nonlinear controllers, such as predictive control and neural network control, are considered an important control method for WPGS in the future. The interaction between WPGS and the grid using nonlinear control strategies and stable operation methods has to be further studied.

The oscillation mechanism analysis and countermeasures of the grid-connected WPGS depend on the prior acquisition of system parameters. With the development of power system intelligence and informatization, oscillating wide-area monitoring and early warning system with the ability to accurately assess system stability in real time and quickly and precisely locate stability weaknesses is one of the keys to establishing a sound and long-lasting operation mechanism for practical engineering and one of the important topics in the direction of stable operation of WPGS on the grid.

In the analysis and damping of HFO at the present stage, WPGS adopts a single-unit model or an equivalent single-unit model with multiple-unit aggregation. This approximation is feasible for large-scale wind farms in the main grid. However, with the large-scale development of distributed new energy sources, multiple WPGS may access the distributed power network widely and dispersedly. Therefore, to address the problem of multiple random variables and complex probability distributions of HFO risk under the trend of diversification of power supply, interaction of power consumption, power electronics and digital intelligence in new power systems, the HFO risk assessment method for new power systems under high-dimensional stochastic conditions needs to be further investigated. Based on the global damping distribution law of the system, the online identification method of weak points affecting system stability can be further explored. In the future, the coupling relationship between the oscillation damping enhancement and the dynamic characteristics of multiple types of regulation resources will be investigated, and the damping remodeling techniques applicable to different regulation resources will be proposed. Combined with the results of stability weak point identification, it is of great significance to study the joint optimization strategy of multiple types of regulation resources for HFO suppression in a new type of power system.

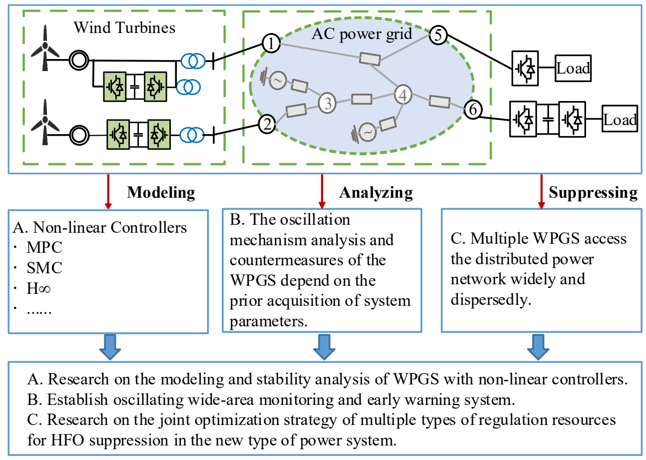

Fig. 8. Outlook for future research on HFO of WPGS.

VI. Conclusion

This paper analyses the HFO occurrence mechanism of the grid-connected WPGS in different scenarios and summarizes the oscillation-inducing factors. The differences between different types of high-frequency oscillation suppression strategies are clarified, and their applicable scenarios are analyzed according to the technical and economic characteristics of various oscillation damping methods. The review and summary of this paper will help researchers and engineers to understand the high-frequency oscillation phenomenon of grid-connected wind turbines in a more in-depth manner so that they can choose appropriate control strategies according to the actual operating conditions, which will have a significant role in promoting the sustained and rapid development of wind power generation.

References

[1] X. Q. He, H. Geng, and G. Mu, "Modeling of Wind Turbine Generators for Power System Stability Studies: a Review," *Renew. and Sustain. Energy Rev.* vol. 143, pp. 110865, Jun. 2021.

[2] X. Xiao, C. Luo, and K. Liao, "Review of the Research on Subsynchronous Oscillation Issues in Electric Power System with Renewable Energy Sources," *Transactions of China Electrotechnical Society*, vol. 32, no. 6, pp. 85–97, Mar. 2017.

[3] V. B. Virulkar, and G. V. Gotmare, "Sub-synchronous Resonance in Series Compensated Wind Farm: a Review," *Renew. and Sustain. Energy Rev.*, vol. 55, pp. 1010–1029, Mar. 2016.

[4] J. Chen, W. J. Du, and H. F. Wang, "A Method of Locating the Power System Subsynchronous Oscillation Source Unit with Grid-connected PMSG Using Deep Transfer Learning," *Transactions of China Electrotechnical Society*, vol. 36, no. 1, pp. 179–190, Jan. 2021.

[5] X. R. Xie, X. Zhang, and H. K. Liu *et al*, "Characteristic Analysis of Subsynchronous Resonance in Practical Wind Farms Connected to Series-compensated Transmissions," *IEEE Trans. on Energy Convers.*, vol. 32, no. 3, pp. 1117–1126, Sept. 2017.

[6] X. R. Xie, Y. Zhan, and J. Shair *et al*, "Identifying the Source of Subsynchronous Control Interaction via Wide-area Monitoring of Sub/super-synchronous Power Flows," *IEEE Trans. on Power Delivery*, vol. 35, no. 5, pp. 2177–2185, Oct. 2020.

[7] C. M. Marc, S. Luis, and P. A. Eduardo *et al*, "Impedance-based Analysis of Harmonic Instabilities in HVDC-connected Offshore Wind

Power Plants," *Int. J. of Electr. Power & Energy Syst.*, vol. 106, pp. 420–431, Mar. 2019.

[8] D. Y. Du, C. Y. Guo, and X. F. Jia *et al*, "Suppression Strategy for High Frequency Resonance of Modular Multilevel Converter Based on Additional Band-stop Filter," *Transactions of China Electrotechnical Society*, vol. 36, no. 7, pp. 1516–1525, Apr. 2021.

[9] E. Ebrahimzadeh, F. Blaabjerg, and X. F. Wang *et al*, "Harmonic Stability and Resonance Analysis in Large PMSG-based Wind Power Plants," *IEEE Trans. on Sustain. Energy*, vol. 9, no. 1, pp. 12–23, Jan. 2018.

[10] X. R. Xie, H. K. Liu, and J. B. He *et al*, "On New Oscillation Issues of Power Systems," *Proc. of the CSEE*, vol. 38 no. 10, pp. 2821–2828+3133, May, 2018.

[11] H. Eroğlu, E. Cuce, and P. M. Cuce *et al*, "Harmonic Problems in Renewable and Sustainable Energy Systems: a Comprehensive Review," *Sustainable Energy Technologies and Assessments*, vol. 48, pp.101566, Dec. 2021.

[12] T. Su, W. Du, and H. Wang, "A Reduced Order Design Method for Subsynchronous Damping Controller of Multi-PMSGs Parallel Wind Farm," *Transactions of China Electrotechnical Society*, vol. 34, no. 1, pp. 116–127, Jan. 2019.

[13] Y. Wang, W. J. Du, and H. F. Wang, "Frequency Drift of Sub-synchronous Oscillation in Wind Turbine Generator Integrated Power System," *Transactions of China Electrotechnical Society*, vol. 35, no. 1, pp. 146–157, Jan. 2020.

[14] S. Li, Y. B. Yan, and X. M. Yuan, "SISO Equivalent of MIMO VSC-dominated Power Systems for Voltage Amplitude and Phase Dynamic Analyses in Current Control Timescale," *IEEE Trans. on Energy Convers.*, vol. 34, no. 3, pp. 1454–1465, Sept. 2019.

[15] G. G. Tu, Y. J. Li, and J. Xiang, "Coordinated Rotor Speed and Pitch Angle Control of Wind Turbines for Accurate and Efficient Frequency Response," *IEEE Trans. on Power Syst.*, vol. 37, no. 5, pp. 3566–3576, Sept. 2022.

[16] S. N. Vukosavic, "Interfacing between the AC Grid and Renewable Power Sources," in *Grid-side Converters Control and Design,* 1st ed., Berlin: Springer, 2018, pp. 110–114.

[17] A. Yazdani, and R. Iravani, *Voltage-sourced Converters in Power Systems: Modeling, Control, and Applications*. New Jersey, USA: John Wiley & Sons, 2010, pp. 215–230.

[18] X. G. Zhang, Y. G. Zhang, and R. Fang *et al*, "An Improved Virtual Inductance Control Method Considering PLL Dynamic Based on Impedance Modeling of DFIG under Weak Grid," *Int. J. of Electr. Power & Energy Syst.*, vol. 118, pp. 105772, Jun. 2020.

[19] S. Golestan, J. M. Guerrero, and J. C. Vasquez, "Three-phase PLLs: a Review of Recent Advances," *IEEE Trans. on Power Electron.*, vol. 32, no. 3, pp. 1894–1907, Mar. 2017.

[20] H. D. Tao, H. T. Hu, and X. J. Zhu *et al*, "High-frequency Damping Analysis and Compensation Method Above Half PWM Sampling Frequency for Train Grid-connected Converter," *IEEE Trans. on Transp. Electrif.*, vol. 8, no. 2, pp. 2945–2958, Jun. 2022.

[21] Y. Y. Xu, H. Nian, and L. Chen, "Small-signal Modeling and Analysis of DC-link Dynamics in Type-IV Wind Turbine System," *IEEE Trans. on Ind. Electron.*, vol. 68, no. 2, pp. 1423–1433, Feb. 2021.

[22] W. H. Zhou, R. E. Torres-olguin, and Y. B. Wang *et al*, "DQ Impedance-decoupled Network Model-based Stability Analysis of Offshore Wind Power Plant under Weak Grid Conditions," *IET Power Electron.*, vol. 13, no. 13, pp. 2715–2729, Oct. 2020.

[23] Y. P. Song, X. F. Wang, and F. Blaabjerg, "Impedance-based High-frequency Resonance Analysis of DFIG System in Weak Grids," *IEEE Trans. on Power Electron.*, vol. 32, no. 5, pp. 3536–3548, May, 2017.

[24] Y. P. Song, and F. Blaabjerg, "Overview of DFIG-based Wind Power System Resonances under Weak Networks," *IEEE Trans. on Power Electron.*, vol. 32, no. 6, pp. 4370–4394, Jun. 2017,

[25] Z. Din, J. Z. Zhang, and Z. Xu *et al*, "Recent Development and Future Trends of Resonance in Doubly Fed Induction Generator System under Weak Grid," *IET Renew. Power Gen.*, vol. 16, no. 5, pp. 807–834, Apr. 2022.

[26] H. Nian, J. Yang, and B. Hu *et al*, "Stability Analysis and Impedance Reshaping Method for Dc Resonance in VSCS-based Power System," *IEEE Trans. on Energy Convers.*, vol. 36, no. 4, pp. 3344–3354, Dec. 2021.

[27] S. Y. Qin, M. X. Yang, and X. G. Zhang *et al*, "Voltage Disturbance Compensation Based on Impedance Modeling of DFIG under Weak Grid," *Int. J. of Electr. Power & Energy Syst.*, vol. 131, pp. 107062, Oct. 2021.

[28] Z. S. Chai, H. Li, and X. J. Xie *et al*, "Output Impedance Modeling and Grid-connected Stability Study of Virtual Synchronous Control-based Doubly-fed Induction Generator Wind Turbines in Weak Grids," *Int. J. of Electr. Power & Energy Syst.*, vol. 126, pp. 106601, Mar. 2021.

[29] H. Tong, H. Nian, and B. Hu *et al*, "High-frequency Resonance Analysis Between DFIG Based Wind Farm with Direct Power Control and VSC-HVDC," in *Proc. of 24th Inter. Confer. on Elec. Mach. and Syst.*, Gyeongju, Korea, Republic of, Oct. 2021, pp. 2207–2212.

[30] J. Pedra, L. Sainz, and L. Monjo, "Comparison of Small-signal Admittance-based Models of Doubly-fed Induction Generators," *Int. J. of Electr. Power & Energy Syst.*, vol. 145, pp. 108654, Feb. 2023.

[31] J. Sun, "Impedance-based Stability Criterion for Grid-connected Inverters," *IEEE Trans. on Power Electron.*, vol. 26, no. 11, pp. 3075–3078, Nov. 2011.

[32] N. Verma, N. Kumar, and R. Kumar, "Battery Energy Storage-based System Damping Controller for Alleviating Sub-synchronous Oscillations in a DFIG-based Wind Power Plant," *Protec. and Cont. of Modern Power Systems*, vol. 8, no. 2, pp. 1–18, Apr. 2023.

[33] K. Wang, X. B. Yuan, and H. Wang *et al*, "Mitigation of Subsynchronous Resonance for Grid-connected Inverters in Series-compensated Weak Power Grids Through Observed Q-axis Grid Voltage Feedback," *IEEE Trans. on Ind. Electron.*, vol. 69, no. 10, pp. 10236–10248, Oct. 2022.

[34] A. M. Tahboub, M. S. E. Moursi, and W. L. Woon *et al*, "Multiobjective Dynamic VAR Planning Strategy with Different Shunt Compensation Technologies," *IEEE Trans. on Power Syst.*, vol. 33, no. 3, pp. 2429–2439, May, 2018.

[35] M. Beza, and M. Bongiorno, "Impact of Converter Control Strategy on Low- and High-frequency Resonance Interactions in Power-electronic Dominated Systems," *Int. J. of Electr. Power & Energy Syst.*, vol. 120, pp. 105978, Sept. 2020.

[36] M. Beza, and M. Bongiorno, "Impact of Converter Control Parameters on the High-frequency Resonance Stability of a Wind-farm Connected to an AC Grid," in *Proc. of EPE '19 ECCE Europe*, Genova, Italy, Sept. 2019, pp. 1–10.

[37] Y. P. Song, F. Blaabjerg, and X. F. Wang, "Analysis and Comparison of High Frequency Resonance in Small and Large Scale DFIG System," in *Proc. of IEEE Ener. Conver. Congre. and Expo.*, Milwaukee, WI, USA, Sept. 2016, pp. 1–8.

[38] L. Zhu, X. G. Hu, and S. Y. Li, "High-frequency Resonance of DFIG-based Wind Generation under Weak Power Network," in *Proc. of 2018 Inter. Confer. on Power Syst. Technology*, Guangzhou, China, Nov. 2018, pp. 2719–2724.

[39] Y. P. Song, and F. Blaabjerg, "Analysis of Middle Frequency Resonance in DFIG System Considering Phase-locked Loop," *IEEE Trans. on Power Electron.*, vol. 33, no. 1, pp. 343–356, Jan. 2018.

[40] B. B. Shao, Q. Xiao, and X. X. Meng *et al*, "Medium-frequency and Sub-synchronous Oscillation Analysis of Direct-drive Wind Farms Connected to the Parallel-compensated AC Grid," *Electric Pow. Syst. Res.*, vol. 216, pp. 109061, Mar. 2023.

[41] B. B. Shao, Z. L. Miao, and L. Y. Wang *et al*, "Participation Factors Weak Robustness Analysis and Mitigation of Direct-drive Wind Farms Connected to the Parallel-compensated Grid," *IEEE Trans. on Energy Convers.*, vol. 38, no. 3, pp. 1924–1936, Sept. 2023.

[42] Y. P. Song, and F. Blaabjerg, "Analysis of the Behavior of Undamped and Unstable High-frequency Resonance in a DFIG System," *IEEE Trans. on Power Electron.*, vol. 32, no. 12, pp. 9105–9116, Dec. 2017.

[43] Y. M. Liao, H. Nian, and M. Li *et al*, "High Frequency Resonance Mechanism and Impedance Reshaping Based on Current Feedback of Three-phased Four-legged Inverter," *Power Syst. Technol.,* vol. 47, no. 1, pp. 83–90, Jan. 2023.

[44] Y. P. Song, N. Heng, and F. Blaabjerg, "Resonance Active Damping and PCC Voltage Quality Improvement of DFIG System Connected to Parallel Compensated Grid," *Chin. J. of Elect. Eng.,* vol. 4, no. 4, pp. 33–40, Dec. 2018.

[45] H. Nian, and B. Pang, "Stability and Power Quality Enhancement Strategy for DFIG System Connected to Harmonic Grid with Parallel

Compensation," *IEEE Trans. on Energy Convers.*, vol. 34, no. 2, pp. 1010–1022, Jun. 2019.

[46] H. Nian, B. Pang, and G. D. Xu *et al*, "Reshaping Strategy of Wide Frequency Impedance for DFIG System to Suppress High Frequency Resonance under Parallel Compensation Grid," *Automation of Electric Power Systems*, vol. 42, no. 18, pp. 48–56, Aug. 2018.

[47] Y. P. Song, H. Nian, and F. Blaabjerg, "High Frequency Resonance in DFIG-based Wind Farm with Variable Power Capacity," *Chin. J. of Elect. Eng*., vol. 3, no. 3, pp. 52–58, Dec. 2017.

[48] Y. P. Song, E. Ebrahimzadeh, and F. Blaabjerg, "Analysis of High-frequency Resonance in DFIG-based Offshore Wind Farm via Long Transmission Cable," *IEEE Trans. on Energy Convers.*, vol. 33, no. 3, pp. 1036–1046, Sept. 2018.

[49] Y. Wu, and P. J. Zhang, "Online Monitoring for Power Cables in DFIG-based Wind Farms Using High-frequency Resonance Analysis," *IEEE Trans. on Sustain. Energy*, vol. 13, no. 1, pp. 378–390, Jan. 2022.

[50] L. W. Dai, H. Wang, and Y. Qin *et al*, "Analysis and Suppression of High-frequency Resonance for Offshore Wind Power Grid-connected Converter Considering Cable Capacitance Effect," *Electronics*, vol. 12 no. 12, pp. 2638, Jun. 2023.

[51] Y. P. Song, E. Ebrahimzadeh, and F. Blaabjerg, "Sensitivity Analysis of the Wind Farm High Frequency Resonance under Transmission Cable Resistance Variation," in *Proc. of APEC*, San Antonio, TX, USA, Mar. 2018, pp. 3218–3224.

[52] R. S. Xie, G. R. Zhang, and B. Xie, "Harmonic Instability Analysis Using State-space Modeling in Grid-connected Inverter System with Long Transmission Cable," in *Proc. of IEEE 6th Inter. Electr. and Ener. Confer.*, Hefei, China, May, 2023, pp. 4392–4398.

[53] Y. Fan, W. Dong, and P. Li *et al*, "Analysis of the Multi-mode Oscillations of Offshore Wind Farms," in *Proc. of 18th Inter. Confer. on AC and DC Pow. Transmission*, Online Conference, China, Jul. 2022, pp. 1657–1663.

[54] Y. P. Song, F. Blaabjerg, and X. F. Wang, "Analysis and Active Damping of Multiple High Frequency Resonances in DFIG System," *IEEE Trans. on Energy Convers.*, vol. 32, no. 1, pp. 369–381, Mar. 2017.

[55] S. Tang, M. Chen, and G. L. Jia *et al*, "Centralized Locating Strategy of Fault Current Limiters in MMC-based Multiterminal HVDC Grid," *IEEE J of Emer. and Sel. Topi. in Pow. Electr.*, vol. 9, no. 6, pp. 7032–7044, Dec. 2021.

[56] R. C. Pan, D. Liu, and Y. X. Yang *et al*, "Network Based Impedance Analysis of Grid Forming Based MMC-HVDC with Wind Farm Integration," *Electric Pow. Syst. Res.*, Vol. 229, pp. 110120, Apr. 2024.

[57] Z. Y. Du, Y. X. Yang, and K. J *et al*, "High Frequency Harmonic Resonance and Suppression in Zhangbei Project," *Power Syst. Technol.*, vol. 46, no. 8, pp. 3066–3075, Aug. 2022.

[58] J. Sun, I. Vieto, and C. Buchhagen, "High-frequency Resonance in HVDC and Wind Systems: Root Causes and Solutions," *IET Renew. Power Gen.*, vol. 17, no. 14, pp. 3507–3522, Sept. 2023.

[59] H. F. Lin, T. Xue, and J. Lyu *et al*, "Impact of Different Ac Voltage Control Modes of Wind-farm-side MMC on Stability of MMC-HVDC with Offshore Wind Farms," *J. of Modern Power Syst. and Clean Energy*, vol. 11, no. 5, pp. 1687–1699, Sept. 2023.

[60] Y. Tan, Y. Sun, and J. H. Lin *et al*, "Revisit Impedance-based Stability Analysis of VSC-HVDC System," *IEEE Trans. on Power Syst.*, vol. 39, no. 1, pp. 1728–1738, Jan. 2024,

[61] F. Dai, D. H. Zeng, and S. Q. Liu *et al*, "A Practical Impedance Modeling Method of MMC-HVDC Transmission System for Medium- and High-frequency Resonance Analysis," *Electric Pow. Syst. Res.*, Vol. 212, pp. 108636, Nov. 2022.

[62] I. Sowa, J. L. Domínguez-García, and O. Gomis-bellmunt, "Impedance-based Analysis of Harmonic Resonances in HVDC Connected Offshore Wind Power Plants," *Electric Pow. Syst. Res.*, vol. 166, pp. 61–72, Jan. 2019.

[63] J. H. Zhu, J. B. Hu, and L. Lin *et al*, "High-frequency Oscillation Mechanism Analysis and Suppression Method of VSC-HVDC," *IEEE Trans. on Power Electron.*, vol. 35, no. 9, pp. 8892–8896, Sept. 2020.

[64] B. Pang, H. Nian, and Y. Y. Xu, "Mechanism Analysis and Damping Method for High Frequency Resonance Between VSC-HVDC and The Wind Farm," *IEEE Trans. on Energy Convers.*, vol. 36, no. 2, pp. 984–994, Jun. 2021.

[65] L. Lin, Q. Q. Zeng, and J. H. Zhu *et al*, "High-frequency Oscillation Mechanism Analysis and Suppression Strategy of Grid-forming Control Mmc-hvdc," *IEEE Trans. on Power Delivery*, vol. 38, no. 3, pp. 1588–1600, Jun. 2023.

[66] Y. F. Li, T. An, and D. Zhang *et al*, "Analysis and Suppression Control of High Frequency Resonance for MMC-HVDC System," *IEEE Trans. on Power Delivery*, vol. 36, no. 6, pp. 3867–3881, Dec. 2021.

[67] M. Amin, and M. Molinas, "Understanding the Origin of Oscillatory Phenomena Observed Between Wind Farms and HVDC Systems," *IEEE J. of Emer. and Sel. Top. in Pow. Electr.*, vol. 5, no. 1, pp. 378–392, Mar. 2017.

[68] Tong Ding, Huaying Zhang, and Hong Xie *et al*, "Network Impedance Reconstruction Method For High-frequency Resonance Mitigation in Cabled Distribution Systems", *Electr. Power Syst. Res.*, vol. 227, Part A, pp. 109968, Feb. 2024.

[69] B. Pang, X. Jin, and X. J. Zhu *et al*, "High Frequency Oscillation Damping for the VSC-HVDC Connects to a Wind Farm via a Cable Transmission Line," *Int. J. of Electr. Power & Energy Syst.*, vol. 147, pp. 108845, May, 2023.

[70] L. Dong, B. Pang, and B. M. Fang *et al*, "Hybrid Impedance Reshaping Based Resonance Damping for the Wind Farm Connected HVDC," in *Proc. of 4th Inter. Confer. on HVDC*, Xi'an, China, Nov. 2020, pp. 349–354.

[71] J. K. Chen, S. Q. Zhu, and R. Q. Wang *et al*, "Analysis and Suppression of Chained SVG High-frequency Resonance in a Cluster Wind Farm System," *Power Sys. Protec. and Contr.*, vol. 51, no. 1, pp. 52–62, Jan. 2023.

[72] J. K. Chen, Q. F. Chang, and X. Hao *et al*, "Analysis of Medium-frequency Oscillation Based on Bifurcation Theory and Joint Modelling of SVG and Direct-drive Wind Turbine," *Int. J. of Electr. Power & Energy Syst.*, vol. 155, pp. 109660, Jan. 2024.

[73] F. Calero, C. A. Cañizares, and K. Bhattacharya, "Dynamic Modeling of Battery Energy Storage and Applications in Transmission Systems," *IEEE Trans. on Smart Grid*, vol. 12, no. 1, pp. 589–598, Jan. 2021.

[74] J. Sun, "Passive Methods to Damp AC Power System Resonance Involving Power Electronics," in *Proc. of IEEE 19th Workshop on Control and Modeling for Pow. Electr.*, Padua, Italy, Jun. 2018, pp. 1–8.

[75] Z. Xu, Y. Q. Jin, and S. X. Li *et al*, "Mechanism Analysis and Mitigation of Harmonic Resonance Amplification Caused by AC Integration of Offshore Wind Farm," *Automation of Electric Power Systems*, vol. 45, no. 21, pp. 85–91, Nov. 2021.

[76] M. J. Yang, D. Y. Li, and X. H. Liu *et al*, "Design of Passive Damping Filter for High-frequency Oscillation Suppression of MMC," in *Proc. of IEEE 2nd International Pow. Electr. and Appli. Sym.*, Guangzhou, China, Nov. 2023, pp. 1531–1535.

[77] R. N. Beres, X. F. Wang, and F. Blaabjerg *et al*, "Optimal Design of High-order Passive-damped Filters for Grid-connected Applications," *IEEE Trans. on Power Electron.*, vol. 31, no. 3, pp. 2083–2098, Mar. 2016.

[78] H. T. Hu, Z. Y. He, and S. B. Gao, "Passive Filter Design for China High-speed Railway with Considering Harmonic Resonance and Characteristic Harmonics," *IEEE Trans. on Power Delivery*, vol. 30, no. 1, pp. 505–514, Feb. 2015.

[79] Y. N. Chi, B. J. Tang, and J. B. Hu *et al*, "Overview of Mechanism and Mitigation Measures on Multi-frequency Oscillation Caused by Large-scale Integration of Wind Power," *CSEE J. of Power and Energy Syst.*, vol. 5, no. 4, pp. 433–443, Dec. 2019.

[80] R. N. Beres, X. F. Wang, M. Liserre *et al*, "A Review of Passive Power Filters for Three-phase Grid-connected Voltage-source Converters," *IEEE J. of Emer. and Sele. Topics in Power Electr.,* vol. 4, no. 1, pp. 54–69, Mar. 2016.

[81] Z. Rafique, H. M. Khalid, and S. M. Muyeen *et al*, "Bibliographic Review on Power System Oscillations Damping: an Era of Conventional Grids and Renewable Energy Integration," *Int. J. of Electr. Power & Energy Syst.*, vol. 136, pp. 107556, Mar. 2022.

[82] Q. H. Liu, C. R. Dong, and Y. M. Yu, "High Frequency Resonance Mechanism and Suppression Strategy of Doubly-fed Wind Power Grid-connected System," *Electric Power Automation Equipment*, vol. 40, no. 9, pp. 163–172, Sept. 2020.

[83] C. Wu, H. Nian, and B. Pang *et al*, "Adaptive Repetitive Control of DFIG-DC System Considering Stator Frequency Variation," *IEEE Trans. on Power Electron.*, vol. 34, no. 4, pp. 3302–3312, Apr. 2019.

[84] J. Lyu, H. F. Lin, and Y. Rao *et al*, "Mechanism and Suppression Control of Wideband Oscillations in MMC-HVDC Connected Offshore Wind Farms," in *Proc. of IPEC-Himeji 2022-ECCE Asia*, Himeji, Japan, May, 2022, pp. 220–224.

[85] Y. P. Song, X. F. Wang, and F. Blaabjerg, "Doubly Fed Induction Generator System Resonance Active Damping Through Stator Virtual Impedance," *IEEE Trans. on Ind. Electron.*, vol. 64, no. 1, pp. 125–137, Jan. 2017.

[86] Z. Din, J. Z. Zhang, and Y. Q. Zhang *et al*, "Active Damping of Resonances in DFIG System with Cascade Converter under Weak Grid," *Inter. Trans. on Electrical Energy Systems*, vol. 29, no. 11, pp. 12118, Nov. 2019.

[87] C. B. Li, D. W. Chen, and J. Wei *et al*, "Parallel Impedance-reshaping Control Strategy for Suppressing Wide Range High-frequency Resonance of Shunt Compensated DFIG System," *IEEE Trans. on Ind. Appl.*, vol. 59, no. 5, pp. 5672–5681, Sept.-Oct. 2023.

[88] H. C. Chen, P. T. Cheng, and X. F. Wang *et al*, "A Passivity-based Stability Analysis of the Active Damping Technique in the Offshore Wind Farm Applications," *IEEE Trans. on Ind. Appl.*, vol. 54, no. 5, pp. 5074–5082, Sept.-Oct. 2018.

[89] K. B. Xu, Y. T. Feng, and Z. Xie *et al*, "Impedance Modeling and Resonance Suppression Strategy of Voltage Source DFIG," in *Proc. of IEEE 16th Confer. on Indu. Electr. and Appli.*, Chengdu, China, Aug. 2021, pp. 637–642.

[90] Z. Din, J. Z. Zhang, and Z. Xu *et al*, "Phase Angle Compensation of Virtual Impedance for Resonance Mitigation in DFIG System under Weak Grid," in *Proc. of 8th Renew. Pow. Generation Confer.*, Shanghai, China, Oct. 2019, pp. 1–8.

[91] M. Matewos, and N. Senroy, "Damping Higher Frequency Resonance of Grid Connected DFIG System," in *Proc. of 2020 IEEE PES/IAS Power Africa*, Nairobi, Kenya, Aug. 2020, pp. 1–5.

[92] Y. P. Song, and F. Blaabjerg, "Wide Frequency Band Active Damping Strategy for DFIG System High Frequency Resonance," *IEEE Trans. on Energy Convers.,* vol. 31, no. 4, pp. 1665–1675, Dec. 2016.

[93] B. Pang, H. Nian, and G. D. Xu *et al*, "Method of Eliminating High Frequency Resonance of DFIG System Connected to Weak Grid," *The Journal of Engineering*, vol. 2017 no. 13, pp. 1793–1798, Dec. 2017.

[94] B. Pang, and H. Nian, "Collaborative Control and Allocation Method of RSC and GSC for DFIG System to Suppress High-frequency Resonance and Harmonics," *IEEE Trans. on Ind. Electron.*, vol. 67, no. 12, pp. 10509–10519, Dec. 2020.

[95] J. Pérez, S. Cobreces, and R. Griñó *et al*, "H_∞ Current Controller for Input Admittance Shaping of VSC-based Grid Applications," *IEEE Trans. on Power Electron.*, vol. 32, no. 4, pp. 3180–3191, Apr. 2017,

[96] R. Chen, J. Zeng, and X. M. Huang *et al*, "An H_∞ Filter Based Active Damping Control Strategy for Grid-connected Inverters with LCL Filter Applied to Wind Power System," *Int. J. of Electr. Power & Energy Syst.*, vol. 144, pp. 108590, Jan. 2023.

[97] S. Cóbreces, X. F. Wang, and J. Pérez *et al*, "Robust Admittance Shaping Approach to Grid Current Harmonic Attenuation and Resonance Damping," *IEEE Trans. on Ind. Appl.*, vol. 54, no. 5, pp. 5039–5053, Sept.-Oct. 2018.

[98] J. Pérez, S. Cóbreces, and R. Griñó *et al*, "Active Damping: an H_∞ Model Reference Approach," *IEEE Trans. on Power Electron.*, vol. 33, no. 8, pp. 7260–7272, Aug. 2018.

[99] Y. Wang, Q. W. Wu, and W. M. Gong *et al*, "H_∞ Robust Current Control for DFIG-based Wind Turbine subject to Grid Voltage Distortions," *IEEE Trans. on Sustain. Energy*, vol. 8, no. 2, pp. 816–825, Apr. 2017.

[100] B. Pang, and H. Nian, "Active Damping Technique Based on H_∞ Controller for VSC under Parallel Compensation Grid," *Electron. Lett.*, vol. 56, no. 3, pp. 147–150, Feb. 2020.

[101] X. F. Wang, Y. W. Li, and F. Blaabjerg *et al*, "Virtual-impedance-based Control for Voltage-source and Current-source Converters," *IEEE Trans. on Power Electron.*, vol. 30, no. 12, pp. 7019–7037, Dec. 2015.

[102] B. Pang, H. Nian, and C. Wu *et al*, "Damping Control of High-frequency Resonance Based on Voltage Feedforward for Voltage Source Converter under a Parallel Compensated Grid," *IET Power Electron.*, vol. 13, no. 13, pp. 2682–2691, Oct. 2020.

[103] L. Rosado, J. Samanes, and E. Gubía *et al*, "Robust Active Damping Strategy for DFIG Wind Turbines," *IEEE Trans. on Power Electron.*, vol. 36, no. 12, pp. 14525–14538, Dec. 2021.

[104] B. Pang, C. Wu, and H. Nian *et al*, "Damping Method of High-frequency Resonance for Stator Current Controlled DFIG System under Parallel Compensation Grid," *IEEE Trans. on Power Electron.*, vol. 35, no. 10, pp. 10260–10270, Oct. 2020.

[105] H. P. Guo, Q. Guo, and T. Y. Guo, *et al*, "Mechanism Analysis and Suppression Method of High Frequency Harmonic Resonance in VSC-HVDC," *Int. J. of Electr. Power & Energy Syst.*, vol. 143, pp. 108468, Dec. 2022.

[106] H. T. Yu, J. Lyu, and X. LI *et al*, "Comprehensive Evaluation of Impact of High-frequency Oscillation Suppression Strategy on the Dynamic Performance of Flexible HVDC Transmission System," *Proc. of the CSEE*, vol. 42, no. 8, pp. 2873–2888, Apr. 2022.

[107] S. Q. Yang, K. P. Liu, and L. Qin, *et al*, "A Broadband Active Damping Method for High-frequency Resonance Suppression in MMC-HVDC System," *Int. J. of Electr. Power & Energy Syst.*, vol. 146, pp. 108791, Mar. 2023.

[108] Z. G. Xu, B. B. Li, and X. Wang *et al*, "High-frequency Resonance Suppression Based on Unified MMC High-frequency Impedance Model," *IEEE Trans. on Power Electron.*, vol. 37, no. 12, pp. 14755–14769, Dec. 2022.

[109] H. L. Xu, C. Z. Liu, and P. J. Ge *et al*, "Hybrid Design of Active and Passive Strategy to Suppress High-frequency Resonances of MMC-based System," *Int. J. of Electr. Power & Energy Syst.*, vol. 157, pp. 109871, Jun. 2024.

Bo Pang (Member, IEEE) was born in Guoyang, China, in 1994. He received the B.Eng. and Ph.D. degrees from the College of Electrical Engineering, Zhejiang University, Hangzhou, China, in 2016 and 2021, respectively.

He is currently an Assistant Professor with the Southwest Jiaotong University, Chengdu, China. His research interests include power quality, stability and enhanced operation control of wind power generation system under non-ideal grid.

Qi Si received the B.S. degree in electronic information engineering from Southwest Jiaotong University, Chengdu, China, in 2022. She is currently working toward the master's degree in electrical engineering with the School of Electrical Engineering, Southwest Jiaotong University, Chengdu.

Her current research interests include stability analysis and control of grid-connected renewable energy system.

Pan Jiang received the B.S. degree in electrical engineering and automation from Southwest Jiaotong University, Chengdu, China, in 2022. He is currently working toward the master's degree in electrical engineering with the School of Electrical Engineering, Southwest Jiaotong University, Chengdu.

His current research interests include power converter control and stability analysis of the power system with power electronic devices.

Kai Liao (Member, IEEE) received the B.E. and Ph.D. degrees in electrical engineering from Southwest Jiaotong University, Chengdu, China, in 2011 and 2016, respectively.

He is currently a Professor at the same university. Previously, he was a Research Fellow with the School of Electrical and Electronic Engineering, Nanyang Technological University, Singapore. His research interests include wind power system control, and power system stability.

Xiaojuan Zhu (Member, IEEE) received the B.S. degree and the Ph.D. degree in electrical engineering from Southwest Jiaotong University, Chengdu, China, in 2015 and 2020, respectively.

From 2018 to 2019, she worked as a visiting doctoral scholar at Technical University of Munich, Germany. She is currently a Postdoctoral Researcher at Southwest Jiaotong University, Chengdu, China. Her main research interests include modeling and control of photovoltaic grid-connected system and designing of a medium-voltage direct current railway electrification system.

Jianwei Yang (Member, IEEE) received the B.S. and Ph.D. degrees in electrical engineering from Southwest Jiaotong University, Chengdu, China, in 2006 and 2011, respectively.

She is currently a Professor with the Department of Electrical Engineering, Southwest Jiaotong University. Her research interests include information theory in electrical power systems, electric power systems fault diagnosis, and fault location.

Zhengyou He (Senior Member, IEEE) received the B.S. and M.S. degrees in computational mechanics from Chongqing University, Chongqing, China, in 1992 and 1995, respectively, and the Ph.D. degree in electrical engineering from the School of Electrical Engineering, Southwest Jiaotong University, Chengdu, China, in 2001.

He is currently a Professor with the School of Electrical Engineering, Southwest Jiaotong University. His research interests include signal process and information theory applied to electrical power systems, and the application of wavelet transforms in power systems.